

# [7–7]- versus [5–5]Bitrovacene: How Linkage Isomerism Affects Exchange Coupling and Redox Splitting<sup>1</sup>

Christoph Elschenbroich,\* Jörn Plackmeyer, Klaus Harms, Olaf Burghaus, and Jürgen Pebler

Fachbereich Chemie der Philipps-Universität, D-35032 Marburg, Germany

Received September 3, 2002

Thermal rearrangement of dicycloheptatriene C<sub>14</sub>H<sub>14</sub> and subsequent reaction with ( $\eta^5$ -cyclopentadienyl)(tetracarbonyl)vanadium affords [7–7]bitrovacene,  $\mu$ - $\eta^7$ : $\eta^7$ -C<sub>14</sub>H<sub>12</sub>[( $\eta^5$ -C<sub>5</sub>H<sub>5</sub>)V]<sub>2</sub> (**8**<sup>••</sup>). Sterically induced avoidance of a planar  $\mu$ - $\eta^7$ : $\eta^7$ -heptafulvalenediyl bridge leads to a complicated packing pattern of varyingly twisted units of **8**<sup>••</sup> which generates a huge unit cell ( $Z = 72$ ), in stark contrast to the isomer **7**<sup>••</sup>, for which  $Z = 2$  applies. The isomers **8**<sup>••</sup> and **7**<sup>••</sup> also differ with regard to the extent of intervanadium electro- and magneto-communication. Redox splittings  $\delta E_{1/2}$  of consecutive ET steps are considerably larger for **8**<sup>••</sup>, compared to **7**<sup>••</sup>, thereby reflecting the higher contribution the larger ring makes to the SOMO. The higher spin density at the C<sub>7</sub> compared to the C<sub>5</sub> carbon atoms, which governs the EPR spectra, effects a pronounced gradation of the exchange coupling parameter determined by magnetic susceptometry:  $J(\mathbf{7}^{\bullet\bullet}) = -2.8$ ,  $J(\mathbf{8}^{\bullet\bullet}) = -24.1$  cm<sup>-1</sup>.

## Introduction

Metal–metal interactions in linked metallocenes (**1**, **2**)<sup>2</sup> have received unflinching attention over the last three decades since the original studies of mixed-valence ferrocene chemistry by Cowan et al.<sup>3</sup> The field has expanded in numerous directions including variation of the central metal atom M, modification of the spacers X between the metallocene units, and application of a multitude of techniques of investigation such as NMR, EPR, UV/vis, IR, XPS, Mössbauer spectroscopy, magnetic susceptometry, and cyclic voltammetry. These endeavors were inter alia driven by the expectation that insights relevant to materials science might accrue. Most examples presented up to now dealt with oligo-sandwich complexes which are connected via the five-membered rings, i.e., in a [5–5] fashion. We had extended the field to [6–6] connectivity by preparing and studying  $\mu$ -( $\eta^6$ : $\eta^6$ -biphenyl)bis[( $\eta^6$ -benzene)chromium] (**3**),<sup>4a</sup> bis- $[\mu$ -( $\eta^6$ : $\eta^6$ -biphenyl)]dichromium (**4**),<sup>4a</sup> and **5**<sup>••</sup>,<sup>4b</sup> the vanadium analogue of **3**. As mentioned recently,<sup>5</sup> an interesting situation is encountered with ( $\eta^7$ -tropylium)vanadium( $\eta^5$ -cyclopentadienyl) (**6**<sup>••</sup>; trovacene<sup>6</sup>) in that three isomeric bitrovacenes, **7**<sup>••</sup>, **8**<sup>••</sup>, and **9**<sup>••</sup>, are conceivable (Scheme 1). This offers an opportunity to compare intermetallic communication mediated by the units  $\mu$ - $\eta^5$ : $\eta^5$ -fulvalenediyl in **7**<sup>••</sup>,  $\mu$ - $\eta^7$ : $\eta^7$ -heptafulvalenediyl in **8**<sup>••</sup>, and  $\mu$ - $\eta^5$ : $\eta^7$ -sesquifulvalenediyl in **9**<sup>••</sup>, respectively, under otherwise identical conditions. In this

paper we report on the synthesis of **8**<sup>••</sup> and its study by X-ray diffraction, EPR, magnetic susceptometry, and cyclic voltammetry. It may be mentioned that complexes containing heptafulvalenediyl (=dicycloheptatrienediyl) bridges  $\mu$ - $\eta^7$ : $\eta^7$ -C<sub>14</sub>H<sub>12</sub> are very scarce,  $\{(\mu$ - $\eta^7$ : $\eta^7$ -C<sub>14</sub>H<sub>12</sub>)-( $\mu$ -I)[Mo(CO)<sub>2</sub>]<sub>2</sub>}PF<sub>6</sub> (**10**) being the only species that has been fully characterized including X-ray diffraction.<sup>7</sup>

## Results and Discussion

**Synthesis.** Lithiation of trovacene proceeds preferentially at the five-membered ring.<sup>8</sup> Therefore, synthesis protocols toward [7–7]bitrovacene **8**<sup>••</sup>, which include functionalization and coupling of mononuclear trovacene units, are impracticable. Rather, a preformed bridging ligand containing two seven-membered rings must be introduced in the final step. Among the conceivable forms **11–13** (Scheme 2) **11** is the most readily accessible one.<sup>9</sup> However, the use of **11** in the standard procedure for the preparation of trovacene **6**<sup>••</sup><sup>10</sup> failed to yield binuclear **8**<sup>••</sup>. Conceivably, the essential dehydrogenation step to yield **8**<sup>••</sup> from the precursor  $\mu$ - $\eta^6$ : $\eta^6$ -**11**[V(C<sub>5</sub>H<sub>5</sub>)<sub>2</sub>] is blocked for steric reasons, the hydrogen

\* To whom correspondence should be addressed. E-mail: eb@chemie.uni-marburg.de.

(1) Trovacene Chemistry. 6. Part 5: Elschenbroich, Ch.; Lu, F.; Harms, K. *Organometallics* **2002**, *21*, 5152.

(2) Barlow, S.; O'Hare, D. *Chem. Rev.* **1997**, *97*, 637.

(3) Cowan, D. O.; Le Vanda, C.; Park, J.; Kaufman, F. *Acc. Chem. Res.* **1973**, *6*, 1.

(4) (a) Elschenbroich, Ch.; Heck, J. *J. Am. Chem. Soc.* **1979**, *101*, 6773. (b) Elschenbroich, Ch.; Heck, J. *Angew. Chem., Int. Ed. Engl.* **1981**, *20*, 267.

(5) Elschenbroich, Ch.; Schiemann, O.; Burghaus, O.; Harms, K.; Pebler, J. *Organometallics* **1999**, *18*, 3273.

(6) By the designation trovacene it is not implied that  $\eta^7$ -C<sub>7</sub>H<sub>7</sub> in **6**<sup>••</sup> should be regarded as a tropylium (C<sub>7</sub>H<sub>7</sub><sup>+</sup>) ion; for recent treatments of bonding conditions in C<sub>7</sub>H<sub>7</sub> complexes see: (a) Green, M. L. H.; Ng, D. K. P. *Chem. Rev.* **1995**, *95*, 439. (b) Fischer, R. D. *Theor. Chim. Acta* **1963**, *1*, 418. (c) Evans, S.; Green, J. C.; Jackson, W. E.; Higginson, E. *J. Chem. Soc., Dalton Trans.* **1974**, 304. (d) Clack, D. W.; Warren, K. D. *Inorg. Chim. Acta* **1978**, *30*, 251. (e) Green, J. C.; Kaltsoyannis, N.; Sze, K. H.; MacDonald, M. *J. Am. Chem. Soc.* **1994**, *116*, 1994. (f) Kaltsoyannis, N. *J. Chem. Soc., Dalton Trans.* **1995**, 3727. (g) Lysenko, K. A.; Antipin, M. Yu.; Ketkov, S. Yu. *Russ. Chem. Bull. Int. Ed.* **2001**, *56*, 130.

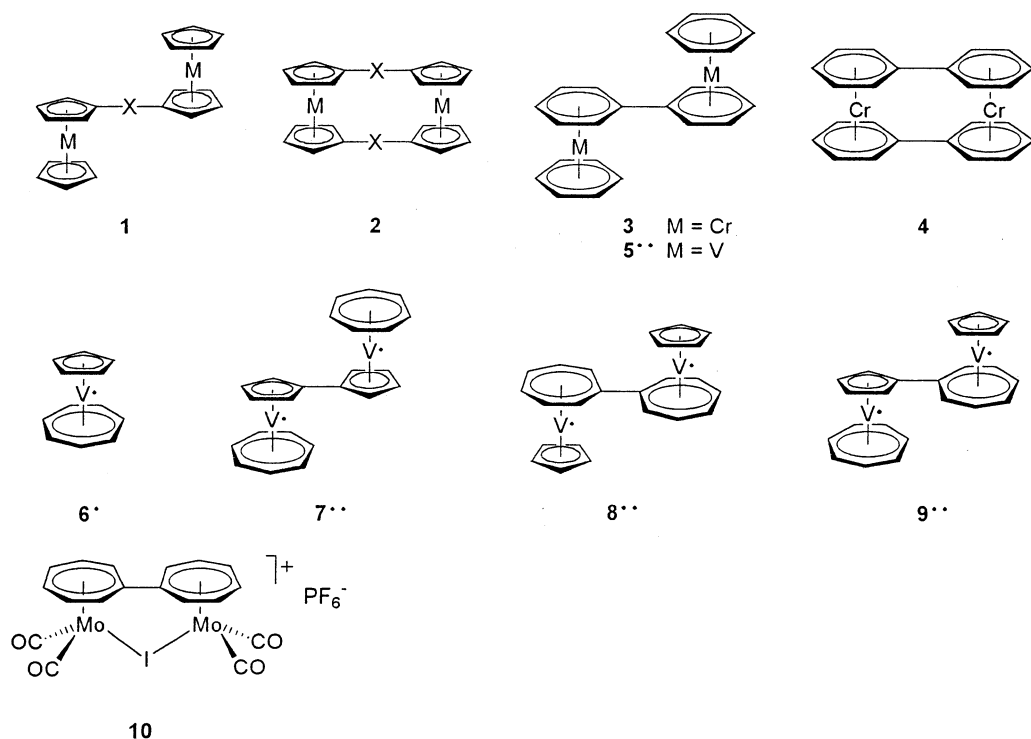
(7) Beddoes, R. L.; Davies, E. S.; Whiteley, M. W. *J. Chem. Soc., Dalton Trans.* **1995**, 3231.

(8) Groenenboom, J. C.; Liefde Meijer, H. J.; Jellinek, F. *Recl. Trav. Chim. Pays-Bas* **1974**, *93*, 6. Groenenboom, J. C.; Liefde Meijer, H. J.; Jellinek, E. *J. Organomet. Chem.* **1974**, *69*, 235.

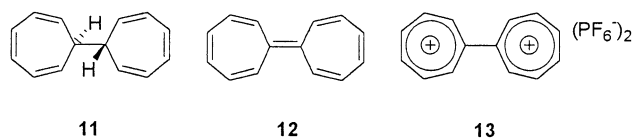
(9) Doering, W. von E.; Knox, L. H. *J. Am. Chem. Soc.* **1957**, *79*, 352.

(10) King, R. B.; Stone, F. G. A. *J. Am. Chem. Soc.* **1959**, *81*, 5263.

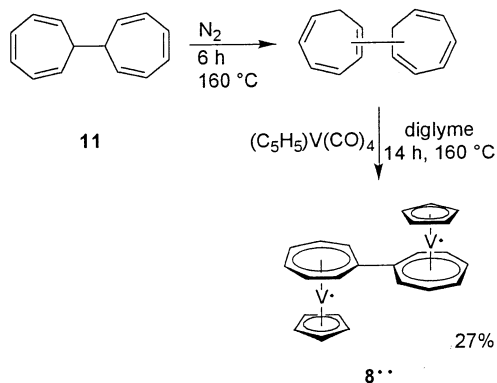
## Scheme 1



## Scheme 2



## Scheme 3



atoms to be removed being bonded to the carbon atoms that link the two seven-membered rings. Inspired by the observation<sup>7</sup> that generation of the dicycloheptatrienyl dication  $\text{C}_{14}\text{H}_{12}^{2+}$  via hydride abstractions from dicycloheptatriene  $\text{C}_{14}\text{H}_{14}$  requires initial thermal isomerization<sup>11</sup> of the latter, we isomerized  $\text{C}_{14}\text{H}_{14}$  prior to the dehydrogenative complexation step (Scheme 3). ( $\mu$ - $\eta^7$ : $\eta^7$ -Heptafulvalenediyl)bis[( $\eta^5$ -cyclopentadienyl)vanadium], [7-7]bitrovacene (**8**), is obtained as blue-violet platelets, which are moderately soluble in benzene, are slightly soluble in diethyl ether, and may be sublimed at 160–170 °C ( $p < 10^{-5}$  mbar).

**X-ray Diffraction.** A stereoplot of the unit cell of **8** is offered in Figure 1; the 10 rotamers of **8** present in the crystal are pictured in Figure 2 together with the respective twist angles and intervannadium distances. The most conspicuous feature of the crystal structure of [7-7]bitrovacene (**8**) is the huge unit cell, which actually contains  $Z = 72$  formula units. This dramatically contrasts with the crystal structure of the isomer [5-5]bitrovacene (**7**), which displays  $Z = 2$ . The reason for this spectacular difference must be searched in structures of the individual molecules. Whereas **7** in the crystal adopts a single trans conformation ( $\theta = 180^\circ$ ), **8** is present in 10 different rotameric forms, none of which corresponding to a trans form. Two synclinal and eight anticlinal rotamers are encountered in the cell which differ in torsional angle and intervannadium distance, as indicated in Figure 2. Obviously, a planar structure of the bridging heptafulvalenediyl ligand is avoided, a fact that we trace to ortho-hydrogen compression strain. Whereas this strain is tolerated in the case of the planar  $\mu$ - $\eta^5$ : $\eta^5$ -fulvalenediyl (**7**) and  $\mu$ - $\eta^6$ : $\eta^6$ -biphenyl (**3**)<sup>12</sup> bridges, the more obtuse intra-ring CCC bond angle in the  $\mu$ - $\eta^7$ : $\eta^7$ -heptafulvalenediyl bridge brings the ortho hydrogen atoms of the neighboring rings into closer proximity, thereby causing a twist distortion. If for the C–H bond length the X-ray crystallographic value of 1.00 Å is chosen, in the planar conformations of the  $\text{C}_n\text{H}_n$ – $\text{C}_n\text{H}_n$  bridges nonbonded H...H distances between ortho/ortho' hydrogen atoms would amount to 2.52 Å ( $n = 5$ ), 1.93 Å ( $n = 6$ ), and 1.44 Å ( $n = 7$ ). In view of the van der Waals radius of the H atoms (1.20–1.45 Å), a planar heptafulvalenediyl bridge would suffer from undue compression strain, which explains its propensity to twist. Twisted conformations of a bridging heptafulvalenediyl ligand have

(11) Volz, H.; Volz-de Lecea, M. *Justus Liebigs Ann. Chem.* **1971**, 750, 136. Bönzli, P.; Neuenschwander, M.; Engel, P. *Helv. Chim. Acta* **1990**, 73, 1685.

(12) Elschenbroich, Ch.; Heck, J.; Massa, W.; Birkhahn, M. *Chem. Ber.* **1990**, 123, 2321.

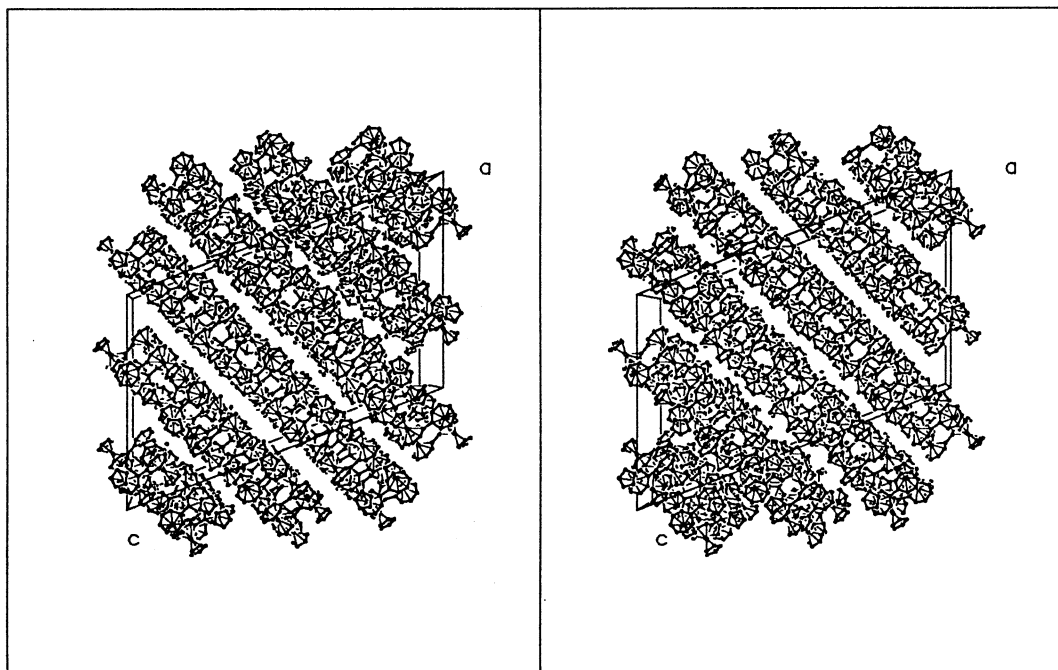


**Figure 1.** Molecular structure of [7-7]bitrovacene ( $\mathbf{8}^{\bullet\bullet}$ ) in the crystal: stereodrawing of the unit cell.

also been established for the complex  $[\text{Mo}_2(\text{CO})_4(\mu\text{-I})(\mu\text{-}\eta^7\text{:}\eta^7\text{-C}_{14}\text{H}_{12})]\text{PF}_6$  ( $\mathbf{10}^7$ ); here the simultaneous presence of an iodine bridge enforces syn conformations exclusively and the twist angles are smaller, amounting to  $35.5^\circ$  and  $39.8^\circ$  in  $\mathbf{10}$  versus  $46^\circ$  and  $50^\circ$  in  $\mathbf{8}$ . Interestingly, the tendency to distort is already apparent for  $(\mu\text{-}\eta^6\text{:}\eta^6\text{-biphenyl})\text{bis}[(\eta^6\text{-benzene})\text{chromium}]$  ( $\mathbf{3}$ ): whereas the inclination to twist is overcome in the single crystal by packing forces, in rigid solution  $\mathbf{3}^{++}$  adopts a twisted structure as demonstrated by the inter-chromium distance derived from the EPR spectra.<sup>4</sup> Increasing propensity to twist-distort is accompanied by increasing C-C bond lengths at the inter-ring junction, which amount to 148.6 pm ( $\mathbf{7}^{\bullet\bullet}$ ), 148.3 ( $\mathbf{3}$ ), and 151–157 pm ( $\mathbf{8}^{\bullet\bullet}$ ), respectively. In concordance with the severely twisted structure of  $\mathbf{8}^{\bullet\bullet}$ , the latter value approaches that of a C-C single bond. The dimensions of the individual trovacene units in  $\mathbf{8}^{\bullet\bullet}$  do not show marked deviations from those of the parent complex  $\mathbf{6}^{\bullet}$ .

**Redox Chemistry.** As depicted in Figure 3, oxidation as well as reduction of  $\mathbf{8}^{\bullet\bullet}$  shows resolved redox-splittings  $\delta E_{1/2}$  ( $2+/+$ ,  $+/0$ ) and  $\delta E_{1/2}$  ( $0/-$ ,  $-/2-$ ), respectively. The cyclic voltammetric data are collected in the caption.

As seems to be the case universally in this class of redox-active binuclear complexes, the  $\delta E_{1/2}$  values for reductions exceed those encountered for oxidations. It has been delineated in a previous paper in this series that electrocommunication between the two metal centers may be triggered by the modulation of the donor/acceptor characteristics of the vanadium atoms caused by the accumulation of negative or positive charge on the latter. This interpretation rests on the fact that, in accordance with the nature of the SOMO in trovacene  $\mathbf{6}^{\bullet}$ , the redox processes are metal-centered. Changes in donor/acceptor character of the vanadium atom engaged in an electron transfer step will then modify the charge on the bridging ligand, thereby influencing the redox potential at the neighboring metal center. As gleaned

from Figure 3, the redox splittings  $\delta E_{1/2}$  ([7-7]trovacene) exceed the values  $\delta E_{1/2}$  ([5-5]trovacene), which amount to  $\delta E_{1/2}$  [( $2+/+$ ), ( $+/0$ )] = 150 mV and  $\delta E_{1/2}$  [( $0/-$ ), ( $-/2-$ )] = 220 mV, respectively. This is rationalized by the fact that the contribution of  $e_2$  metal-ligand back-bonding increases with ring size<sup>6a</sup> and, correspondingly, transmission efficiency of electronic effects increases. The larger  $\delta E_{1/2}$  values for reductions, relative to oxidations, fit the same picture in that metal-ligand overlap is expected to be larger for metal orbitals bearing a negative rather than a positive charge. The comproportionation constant for the equilibrium  $\mathbf{8}^{\bullet\bullet} + \mathbf{8}^{2-} \rightleftharpoons 2 \mathbf{8}^{\bullet}$  calculated by means of the relation  $K_c = \exp(\delta E_{1/2} n F / RT)$ ,<sup>13</sup> inserting the value  $\delta E_{1/2}$  [( $0/-$ ), ( $-/2-$ )] = 0.33 V, amounts to  $K_c(238 \text{ K}) = 7.5 \times 10^6$ . The value of  $K_c$  places  $\mathbf{8}^{\bullet}$  in the class of delocalized intermediate valence species that should be accessible on a preparative scale. This will require reduction of  $\mathbf{8}^{\bullet\bullet}$  at the controlled, highly cathodic potential of  $\approx -2.5$  V and is a topic of future investigation.

**EPR Spectroscopy.** Not unexpectedly, the EPR spectrum of  $\mathbf{8}^{\bullet}$  in fluid solution (Figure 4) points to an exchange coupling constant  $J$  which largely exceeds the hyperfine coupling constant  $a(^{51}\text{V}, \mathbf{6}^{\bullet})$ . This is to be concluded from the hyperfine pattern, which consists of 15 lines in the correct binomial intensity distribution for coupling to two magnetic nuclei  $^{51}\text{V}$  ( $I = 7/2$ ). While in this respect  $\mathbf{8}^{\bullet}$  mimics  $\mathbf{7}^{\bullet}$ , the rigid solution spectra differ in that the half-field signal ( $\Delta M_s = 2$ ), which is indicative of biradical character, is considerably stronger for  $\mathbf{8}^{\bullet}$  than for  $\mathbf{7}^{\bullet}$ . As opposed to  $\mathbf{7}^{\bullet}$ , where spectral accumulation was called for, the half-field signal of  $\mathbf{8}^{\bullet}$  is barely detectable as part of the original unamplified trace. This observation indicates that electron spin dipolar coupling in [7-7]bitrovacene markedly exceeds that exhibited by its isomer [5-5]bitrovacene. It has been shown that the ratio of the intensity of the

(13) Richardson, D. E.; Taube, H. *Coord. Chem. Rev.* **1984**, *60*, 107.

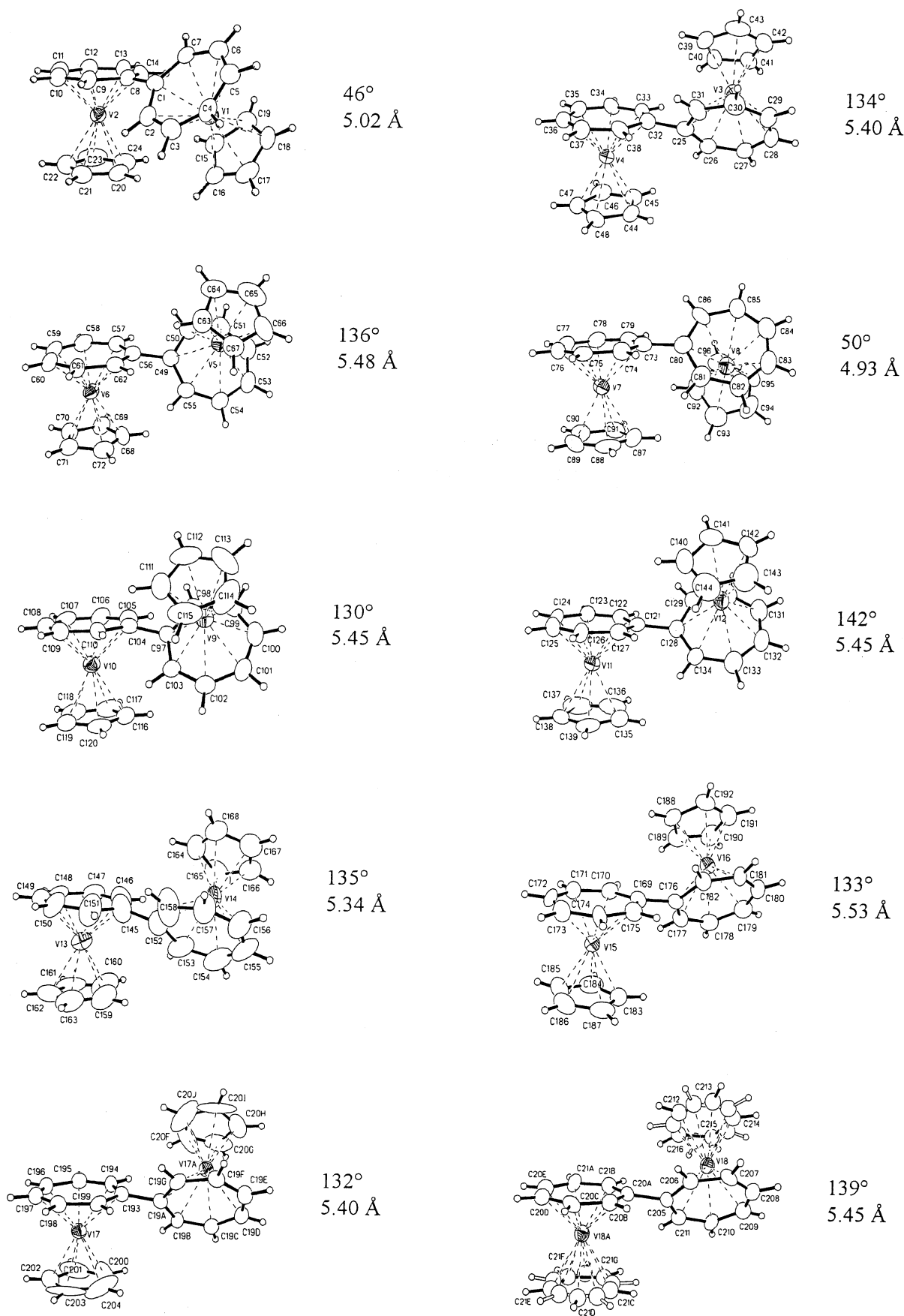


**Figure 2.** Molecular structure of [7-7]bitrovacene (**8\*\***) in the crystal: views of the 10 different rotamers present in the unit cell with the respective intersandwich twist angles  $\theta$  (deg) and intramolecular intervandium distances V...V (Å). The thermal ellipsoids are drawn at a 50% probability level. Individual bond distances and bond angles for the trovacene units are collected in the Supporting Information.

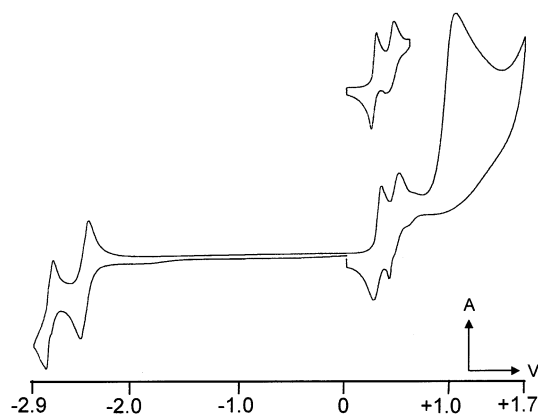


**Figure 3.** Cyclic voltammogram of [7-7]bitrovacene (**8\*\***) in DME/ $\text{Bu}_4\text{NClO}_4$  at  $-35\text{ }^\circ\text{C}$  and  $\nu = 100\text{ mV/s}$  vs SCE.  $E_{\text{pa}} = 1.07\text{ V}$ ;  $E_{1/2}(2+/+) = 0.45\text{ V}$ ,  $\Delta E_{\text{p}} = 110\text{ mV}$ ,  $r = 1$ ;  $E_{1/2}(+/0) = 0.29\text{ V}$ ,  $\Delta E_{\text{p}} = 80\text{ mV}$ ,  $r = 1$ ;  $\delta E_{1/2}[(2+/+), (+/0)] = 160\text{ mV}$ ;  $E_{1/2}(0/-) = -2.41\text{ V}$ ,  $\Delta E_{\text{p}} = 80\text{ mV}$ ,  $r = 1$ ;  $E_{1/2}(-/2-) = -2.74\text{ V}$ ,  $\Delta E_{\text{p}} = 63\text{ mV}$ ,  $r = 1$ ;  $\delta E_{1/2}[(0/-), (-/2-)] = 330\text{ mV}$ . Inset: scan between 0 and 0.6 V (vs SCE), showing the first two oxidation waves.  $E_{\text{pa}}$  = anodic peak potential;  $\Delta E_{\text{p}}$  = peak separation;  $E_{1/2}$  = half-wave potential;  $r = i_{\text{a}}/i_{\text{c}}$  (current ratio);  $\delta E_{1/2}$  = redox splitting.

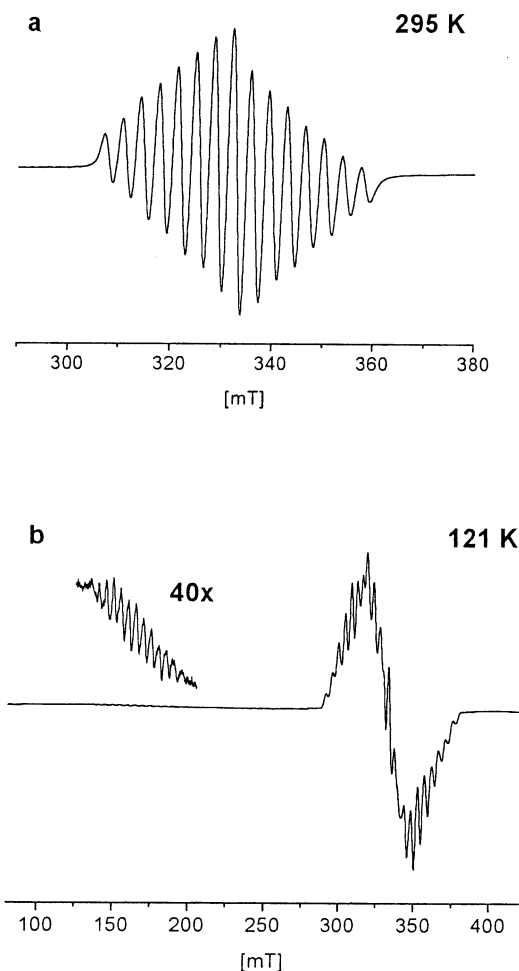


**Figure 4.** EPR spectra (X-band) of [7-7]bitrovacene (**8\*\***) in toluene: (a) fluid solution; (b) rigid solution.  $\langle g \rangle = 1.9832$ ,  $a(^{51}\text{V}) = -7.19\text{ mT}$ . From the splitting of  $5.0\text{ mT}$  in the  $\Delta M_s = 2$  multiplet,  $A_{\perp}(^{51}\text{V}) = -10.0\text{ mT}$  is derived.

forbidden half-field transition ( $\Delta M_s = 2$ ) to that of the allowed transition ( $\Delta M_s = 1$ ) depends on the value of the interspin distance  $r$  and is independent of the

magnitude of the exchange coupling constant  $J$ .<sup>14</sup> Therefore the relative intensities of the half-field signals for **7\*\*** and **8\*\*** suggest that electron spin dipolar coupling is stronger in the latter. This may be explained by the fact that the avoidance of a strict trans conformation in the case of the [7-7] isomer **8\*\*** places the spin bearing vanadium atoms in closer proximity as compared to the [5-5] isomer **7\*\***, where the trans conformation is accessible (see the X-ray structural results). Since in the present class of compounds, because of the very small  $g$ -anisotropy ( $\Delta g \approx 0.02$ ), anisotropic exchange can be neglected, dipolar coupling may be regarded as the sole contributor to zero-field splitting. Therefore, based on the point-dipole approximation, the magnitude of the zero-field splitting parameter  $D$  furnishes information on the mean interspin distance.  $D$  can be extracted from the rigid-solution EPR spectrum of **8\*\***, the total width of which amounts to  $2D + 14/2 A_{\perp}(^{51}\text{V})$ . The value of  $D = 185\text{ G}$  ( $0.0173\text{ cm}^{-1}$ ) thus obtained and use of the relation  $D = 0.65g_{\perp}^2/r^3$ <sup>15</sup> yields the value  $r = 5.29\text{ \AA}$  for the interspin distance in **8\*\***. This value conforms with the mean inter-vanadium distance ( $5.34\text{ \AA}$ ) of the conformers present in the unit cell of **8\*\***. Interestingly, the inter-vanadium distances, derived in the same way for  $\mu$ -( $\eta^6$ : $\eta^6$ -biphenyl)bis[( $\eta^6$ -benzene)vanadium]**5\*\*** and [5-5]bitrovacene **7\*\***, amount to  $5.40$  and  $5.70\text{ \AA}$ , respectively. As indicated by the results of the structure determination, the readiness to adopt a precise trans conformation decreases with increasing ring size in the bridging unit, i.e.,  $\text{C}_5\text{H}_4\text{C}_5\text{H}_4 > \text{C}_6\text{H}_5\text{C}_6\text{H}_5 > \text{C}_7\text{H}_6\text{C}_7\text{H}_6$ ; accordingly **8\*\***, the complex with the largest rings in the bridge, features the smallest mean inter-vanadium distance, a result that had already been gleaned from the relative intensities of the half-field signals in the EPR spectra.

**Magnetic Susceptibility.** Since the exchange coupling constant  $J(\mathbf{8**})$  lies outside the range accessible via an analysis of the  $a(^{51}\text{V})$  hyperfine pattern, magnetic susceptometry must be applied. The temperature dependence of the susceptibility  $\chi(\mathbf{8**})$  is shown in Figure 5.  $\chi$  passes through a maximum at  $26\text{ K}$ , falls to a minimum at  $5\text{ K}$ , and rises again for  $T < 5\text{ K}$ . This behavior requires the use of a modified Bleaney–Bowers relation<sup>16b</sup>

$$\chi_{\text{m}} = \frac{2Ng^2\mu_{\text{B}}^2}{k(T - \Theta)[3 + \exp(-J/kT)]} (1 - \rho) + \frac{Ng^2\mu_{\text{B}}^2}{2kT}\rho$$

With regard to the basic expression<sup>16a</sup>  $\chi_{\text{m}} = 2Ng^2\mu_{\text{B}}^2 \{kT[3 + \exp(-J/kT)]\}^{-1}$  the modifications account for intermolecular magnetic interactions by the parameter  $\Theta$  and for traces of noncoupled species in the sample by their mole fraction  $\rho$ . The impurity is assumed to follow the Curie law. Least-squares fitting is accomplished with the parameters  $J = -24.1\text{ cm}^{-1}$ ,  $\Theta = -10.25\text{ K}$ ,  $\rho = 0.0079$ ; the value  $g = 1.9832$  was taken from the EPR spectrum. Employing the Curie–Weiss law in the higher temperature range ( $T > 55\text{ K}$ ) furnishes the Weiss constant  $\Theta_{\text{w}} = -25.20\text{ K}$ , and a

(14) Eaton, S. S.; More, K. M.; Sawant, B. M.; Eaton, G. R. *J. Am. Chem. Soc.* **1983**, *105*, 6560.

(15) Belford, R. L.; Chasteen, N. D. *Inorg. Chem.* **1970**, *9*, 169.

(16) (a) Bleaney, B.; Bowers, K. D. *Proc. R. Soc. (London) Ser. A.* **1952**, *214*, 451. (b) Kahn, O. *Molecular Magnetism*, VCH: Weinheim, 1993; p 107.

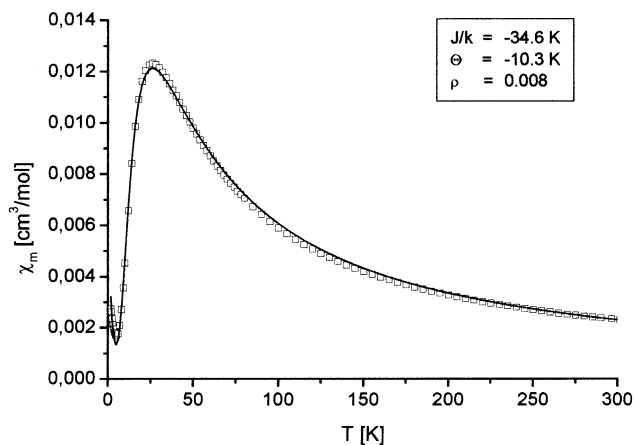


**Figure 5.** Magnetic susceptibility data for [7-7]bitrovacene (**8\*\***) at 30 kG in the temperature range 1.8–300 K ( $\square$ ). The solid line represents the best fit to the Bleaney–Bowers expression (see text) with  $J = -24.1 \text{ cm}^{-1}$ ,  $\Theta = -10.3 \text{ K}$ , and  $\rho = 0.008$ .

magnetic moment per vanadium atom,  $\mu_V = 1.72\mu_B$ , which approaches the free spin value.

A striking result is the magnitude of the exchange coupling constant for [7-7]bitrovacene,  $J(\mathbf{8}^{**}) = -24.1 \text{ cm}^{-1}$ , which exceeds the value for the isomer [5-5]trovacene,  $J(\mathbf{7}^{**}) = -2.78 \text{ cm}^{-1}$ ,<sup>5</sup> by a factor of 8.6. A clue to this finding is provided by the strongly differing spin densities at the ipso-carbon atoms of the five- and seven-membered ring of parent **6\***. Contact-shift <sup>1</sup>H NMR and EPR measurements and their assignment, aided by deuteration of the cyclopentadienyl ligand, had yielded the isotropic hyperfine parameters  $a(\mathbf{6}^*, 7 \text{ } ^1\text{H}) = 0.43 \pm 0.02 \text{ mT}$  (NMR),  $0.48 \pm 0.03 \text{ mT}$  (EPR) and  $a(\mathbf{6}^*, 5 \text{ } ^1\text{H}) = 0.18 \pm 0.01 \text{ mT}$  (NMR).<sup>17</sup> These data reflect the spin transfer from the SOMO  $V(3d_z^2)$  into the 1s orbitals of the peripheral H atoms. Spin coupling of the two vanadium-centered unpaired electrons in [7-7]bitrovacene **8\*\*** via a superexchange mechanism must be mediated by the C–C bond connecting the two trovacene moieties. Irrespective of the intimate mechanism—spin polarization of the  $\sigma$ - or  $\pi$ -bond between the two ipso-carbon atoms—it is plausible that the efficiency of this interaction should be proportional to the spin densities prevailing at the linking atoms. This notion gives rise to the ratio  $[a(^1\text{H}, C_7)]^2/[a(^1\text{H}, C_5)]^2 = 4.5^2/1.8^2 = 6.25$ , which closely resembles the ratio of the exchange coupling constants,  $J(\mathbf{8}^{**})/J(\mathbf{7}^{**}) = 8.6$ . Admittedly, this crude model suffers from the noninclusion of conformational preferences, a quite serious deficiency in view of the fact that here we correlate fluid solution spectroscopic data (isotropic hyperfine coupling) with a solid state property (bulk magnetic susceptibility), although the conformations in the different phases may vary considerably. While in the form of the relation  $J[m-n] \approx C \cdot a(^1\text{H}_m) \cdot a(^1\text{H}_n)$  may be rationalized as discussed above, the value of the proportionality constant,  $C \approx 1$  if  $J$  is expressed in  $\text{cm}^{-1}$  and  $a(^1\text{H})$  in Gauss, is fortuitous. It is tempting to use this simple relation to predict exchange coupling constants  $J$  for other directly connected intersandwich complex biradicals for which EPR hyperfine data of the building blocks are known.

**Table 1. Crystal Data and Structure Refinement for (**8\*\***)**

Crystal Data	
identification code	multiscan
habit, color	plate, green/red
cryst size	$0.32 \times 0.25 \times 0.08 \text{ mm}^3$
cryst syst	monoclinic
space group	$C2/c$ , $Z = 72$
unit cell dims	$a = 45.919(3) \text{ \AA}$ , $\alpha = 90^\circ$ $b = 26.4287(10) \text{ \AA}$ , $\beta = 111.351(5)^\circ$ $c = 29.233(2) \text{ \AA}$ , $\gamma = 90^\circ$
volume	$33041(3) \text{ \AA}^3$
cell determination	32 361 reflns
empirical formula	$C_{24}H_{22}V_2$
fw	412.30
density (calcd)	$1.492 \text{ Mg/m}^3$
abs coeff	$1.022 \text{ mm}^{-1}$
$F(000)$	15 264
Data Collection	
diffractometer type	IPDS2
wavelength	$0.71073 \text{ \AA}$
temperature	$193(2) \text{ K}$
$\theta$ range for data collection	$1.28\text{--}25.00^\circ$
index ranges	$-52 \leq h \leq 53$ , $-31 \leq k \leq 31$ , $-34 \leq l \leq 34$
data collection software	STOE Win-Xpose (X-Area)
cell refinement software	STOE Win-Cell (X-Area)
data reduction software	STOE Win-Integrate (X-Area)
Solution and Refinement	
no. of reflns collected	107 227
ind reflns	27 978 [ $R(\text{int}) = 0.0995$ ]
completeness to $\theta = 25.00^\circ$	96.1%
obsd reflns	10 849 [ $I > 2\sigma(I)$ ]
no. of reflns used for refinement	27 978
abs corr	semiempirical from equivalents
max. and min. transmn	0.9227 and 0.7357
largest diff peak and hole	0.633 and $-0.430 \text{ e \AA}^{-3}$
solution	direct methods
refinement	full-matrix least-squares on $F^2$
treatment of hydrogen atoms	calcd, $U_{\text{iso}}(\text{H}) = 1.2 U(\text{eq})C$
programs used	SHELXS-97 (Sheldrick, 1990) SHELXL-97 (Sheldrick, 1997) SHELXTL, STOE IPDS software
no. of data/restraints/params	27978/472/2094
goodness-of-fit on $F^2$	0.763
$R$ index (all data)	wR2 = 0.1204
$R$ index conventional [ $I > 2\sigma(I)$ ]	R1 = 0.0572

Thus, employing the hyperfine coupling constant  $a[^1\text{H}, (\text{C}_6\text{H}_6)_2\dot{\text{V}}] = 4.05 \text{ G}$ ,<sup>4</sup> for the biradical **5\*\*** the value  $|J|(\mathbf{5}^{**}) = 16.40 \text{ cm}^{-1}$ , and using the hyperfine coupling constants of **6\***, for [5-7]bitrovacene **9\*\*** the value  $|J|(\mathbf{9}^{**}) = 8.1 \text{ cm}^{-1}$  is anticipated. Accordingly, exchange interaction is expected to be mediated about twice as extensively by the symmetrical  $\mu\text{-}\eta^6\text{:}\eta^6\text{-biphenyl}$  bridge as compared to the isomeric unsymmetrical  $\mu\text{-}\eta^5\text{:}\eta^7\text{-sesquifulvalenediyl}$  bridge. This prediction will have to be verified by magnetic susceptometry on the known complex **5\*\***<sup>4</sup> and by the synthesis and study of the unknown isomer **9\*\***.

## Experimental Section

All chemical manipulations were performed with exclusion of air under dinitrogen or argon (CV). Physical measurements

(17) Rettig, M. F.; Stout, C. D.; Klug, A.; Farnham, P. *J. Am. Chem. Soc.* **1970**, *92*, 5100.

were carried out using instruments specified previously.<sup>18</sup> Magnetic susceptibility was studied with a SQUID susceptometer (Quantum Design) in the temperature range 1.8–300 K. The data were corrected for magnetization of the sample holder (KLF), and diamagnetic corrections were applied to the magnetic susceptibility data based on Pascal's constants. CpV(CO)<sub>4</sub><sup>19</sup> and 7,7-dicycloheptatriene (C<sub>14</sub>H<sub>14</sub>, **11**)<sup>9</sup> were prepared as described in the literature. Thermal isomerization of 7,7-dicycloheptatriene was carried out according to ref 11.

**[7-7]Bitrovacene (8<sup>\*</sup>)**. ( $\eta^5$ -Cyclopentadienyl)vanadium-(tetracarbonyl) (1.45 g, 6.36 mmol) and thermally rearranged dicycloheptatriene (0.58 g 3.18 mmol) were dissolved in 20 mL of diglyme and heated to 150–160 °C over a course of 50 min, during which the onset of gas evolution was noted together with a color change from red to greenish-brown. The mixture was stirred at 150–160 °C for 14 h. After cooling to room temperature the solvent was removed at reduced pressure, yielding a dark residue, which was redissolved in 5 mL of benzene and passed through a short column (3 × 10 cm) of Al<sub>2</sub>O<sub>3</sub> (2% H<sub>2</sub>O). The resulting blue-green solution was reduced in vacuo to 5 mL and subjected to column chromatography on Al<sub>2</sub>O<sub>3</sub> (0% H<sub>2</sub>O, 3 × 22 cm, benzene). The first zone, a blue-green solution, was stripped to 5 mL and stored for several days at 4 °C to form blue-violet platelets. Yield: 0.36 g (0.87 mmol, 27%) of [7-7]bitrovacene **8<sup>\*</sup>**. Single crystals suitable for X-ray diffraction were grown at 4 °C from DME. MS (EI, 70 eV): *m/z* (relative intensity) 412 (M<sup>+</sup>, 100), 207 (C<sub>12</sub>H<sub>12</sub>V<sup>+</sup>, 28), 153 (C<sub>12</sub>H<sub>9</sub><sup>+</sup>, 9), 129 (C<sub>6</sub>H<sub>6</sub>V<sup>+</sup>, 6), 116 (C<sub>5</sub>H<sub>5</sub>V<sup>+</sup>, 46), 107 (C<sub>8</sub>H<sub>7</sub><sup>+</sup>, 10), 91 (C<sub>7</sub>H<sub>7</sub><sup>+</sup>, 9), 51 (V<sup>+</sup>, 7). IR (KBr, cm<sup>-1</sup>): 3027 w, 1491 w, 1474 w, 1421 w, 1108 m, 1006 s, 965 m, 903 m, 851 m, 817 m, 784 br, vs, 686 s, 423 br, s. Anal. Calcd for C<sub>24</sub>H<sub>22</sub>V<sub>2</sub> (412.32): C, 69.91; H, 5.38. Found: C, 69.21; H 5.40. For EPR, CV, and magnetic susceptometry see text.

(18) Elschenbroich, Ch.; Voss, S.; Schiemann, O.; Lippek, A.; Harms, K. *Organometallics* **1998**, *17*, 4417.

(19) Floriani, C.; Del Nero, S.; Fachinetti, G. *J. Chem. Soc., Dalton Trans.* **1976**, 1046.

**X-ray Crystallographic Study of 8<sup>\*</sup>**. Crystal data and technical details of the determination are listed in Table 1. Data were collected at 193 K on a STOE IPDS-2 diffractometer using Mo K $\alpha$  radiation and corrected for absorption using the intensities of equivalent reflections (transmission factors 0.92 and 0.74). The structure was solved using direct methods and refined on *F*<sup>2</sup> values using the full matrix least-squares method. A 2-fold disorder of the five-membered ring of the molecule containing V(18) has been refined using restraints. Unusual temperature factors indicate a similar disorder of the molecule containing V(17) that has not been refined. The hydrogens have been placed on calculated positions and refined using a riding model with  $U_{\text{iso}}(\text{H}) = 1.2U(\text{eq})\text{C}$ . Programs used: SHELXS-97 and SHELXL-97 (G. M. Sheldrick, University of Göttingen, Germany, 1997), STOE X-Area 1.16 (STOE & CIE GmbH, Darmstadt, Germany, 2002), SHELXTL 5.02 (Siemens Analytical X-ray Instruments Inc., Madison, WI, 1996), WinGX v1.64.04 (L. J. Farrugia, *J. Appl. Crystallogr.* **1999**, *32*, 837–838), PLATON (A. L. Spek, Utrecht University, Utrecht, The Netherlands, 2002).

**Acknowledgment.** This work has been supported by the Volkswagen Foundation, the Deutsche Forschungsgemeinschaft, and the Fonds der Chemischen Industrie. We are indebted to Professor W. Massa for helpful comments. For technical assistance we thank Ms. A. Nagel.

**Supporting Information Available:** Tables giving crystal data and details of the structure determination, positional and thermal parameters, and all bond distances and angles for **8<sup>\*</sup>**. This material is available free of charge via the Internet at <http://pubs.acs.org>.

OM020717Q